Boxprop, a forward-swept joined-blade propeller

Richard Avellán & Anders Lundbladh
GKN Aerospace Sweden
SE-46181 Trollhättan, Sweden

Abstract

This article describes the Boxprop, a new high-speed propeller concept with forward swept joined-blades for future transport aircraft applications. Both numerical and experimental investigations of the joined-blade propeller were carried out at GKN Aerospace and Chalmers University in order to answer some of the fundamental questions relating to aerodynamic performance and mechanical integrity. The results show that the Boxprop concept works as intended and in particular that rapid prototyping methods using polymeric materials are suitable for early product development, even for functional testing of high speed propellers.

Furthermore, based on the positive outcome of the experimental work described in this article, the next development step can be started by initiating the design of the counter-rotating Boxprop and wind tunnel test stand to proof the concept at TRL 3.

Nomenclature

AF Activity factor,

$$AF = \frac{10^5}{16} \int_{\frac{R_h}{R_t}}^{1.0} \frac{c}{D}\left(\frac{R}{R_t}\right)^3 d\left(\frac{R}{R_t}\right) n$$

COTS	Commercial Off-The-Shelf
c	blade chord [m]
C_T	Thrust coefficient, $T/\rho N^2 D^4$
D	Propeller diameter [m]
FDM	Fused Deposition Modeling
FE	Finite Element
GPS	GKN Propeller, Single-blade
GPX	GKN Propeller, boX blade
J	Advance ratio, V/ND
M	Mach number [-]
N	Rotational speed [rps]
n	Number of blades
N/A	Not Available
Pitch	Blade angle at 75% radius
R	Radius [m]
T	Thrust [N]
TRL	Technology Readiness Level
UTS	Ultimate Tensile Strength
V	Free-stream velocity [m/s]
ρ	Air density [kg/m^3]

Subscripts

h	hub
t	tip

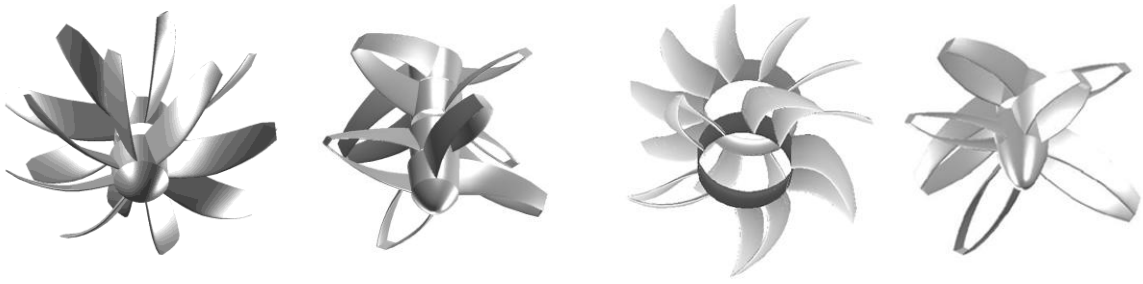

Figure 1. Examples of high-speed propeller concepts.
The conventional counter-rotating propeller is shown to the left.

Introduction

One of the most promising technical innovations for reducing aircraft fuel consumption within the next 20 years is the introduction of aero engines with counter-rotating high speed propellers, e.g. open rotors.

A drawback with the counter-rotating open rotor is the increased noise it may generate, at least in comparison with a future generation ducted ultra high bypass engine integrated in a conventional noise attenuating nacelle. The open rotor noise is to a great extent caused by the interaction of the wake of the forward propeller with the aft one. Also the weight of the open rotor engine and the reduced fan efficiency caused by exposure to the full flight speed, somewhat reduce the effect of the improved propulsive efficiency.

A propeller blade, just as an aircraft wing, generates a tip vortex, which is associated with the blade's induced drag and also contributing to increased noise when interacting with the aft propeller. It is well known that winglets and double wings joined at the tip (a box wing) can reduce the tip vortex local strength and also decrease wing induced drag[1,2]. This effect can consequently be of interest also for propeller design. Such a blade pair joined at the tips can in the same manner be referred to as a box blade.

Further there is some evidence that a forward swept propeller may enjoy a tip flow less compromised by boundary layer effects. Considering simple sweep theory for aircraft wings it might not seem obvious that sweeping a wing forwards would give any additional benefits compared to the same amount of rearward sweep. However, for reasons similar to those resulting in the flight test program X-29[3] and have resulted in more recent research related to subsonic transport aircraft[4,5] it is observed that forward swept wings still have a very interesting potential aerodynamic benefit that also should be investigated further for propellers.

For a counter-rotating propeller pair the increased axial separation between the tips of the forward and rear propeller reduces the strength of the forward blade wake where it arrives at the rear blade which has beneficial impact on the interaction noise[6]. However, forward swept, thin bladed propellers are prone to aerodynamic instability and flutter[7]. To exploit these improvements to propeller aerodynamics a double bladed high speed propeller has been proposed, see figure 1 and 2.

The box blades are stiffer and may allow a flutter free forward swept design that also most likely is stronger in the case of a bird impact. By suitable shaping of the blades the centrifugal force is carried by tensile stresses, avoiding excessive bending and high stress concentrations. An initial design study shows that the stacking line therefore must approximate a rotating catenary. To avoid a bending moment in the blade stub shaft, the inner portion of the blade must have rearward sweep smoothly changing to a forward swept outer portion. This also reduces leading and trailing edge stresses, although some stress concentration remains where the sweep changes direction.

For a counter-rotating propeller pair various combinations of forward and rearward sweep, single- and joined-blade propellers are possible, see figure 1.

The properties of a joined-blade propeller are still relatively unknown, and there are both aerodynamic and mechanical issues which need to be understood to assess its full development potential.

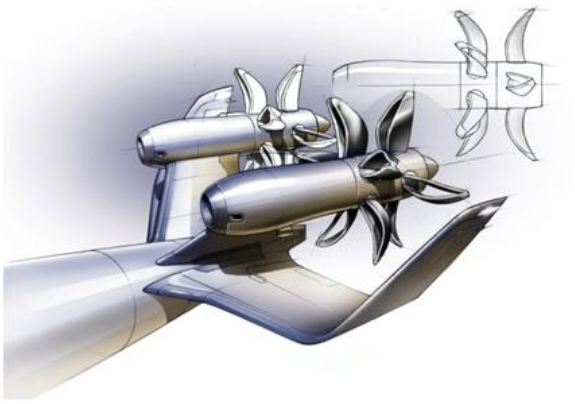

Figure 2. Artist's impression of a joined-blade propeller.

Joined-blade propeller background

The first publication describing the joined-blade propellers presented in this study was the patent application filed by the authors in 2009[8,9]. Wingtip-devices for general aviation propellers, so called proplets, have been studied before and the results indicate a potential noise reduction and propeller efficiency increase, see for instance the reports by Korkan[10] and Jeracki[11]. Moreover, Hartzell Propeller in the U.S. offers aluminum propellers for rated powers up to 700 hp with "q-tips" which is a 90 degree bent tip section that reduces the noise levels according to the manufacturer[12].

In figure 3 the potential ideal aerodynamic benefit stemming from the induced drag reduction of several different joined-wings is shown. From the study by Kroo[2] it is also worth noting that adding a winglet device to the planar wing is almost as efficient as a box-wing configuration but is lacking the mechanical benefits of the closed box-wing system.

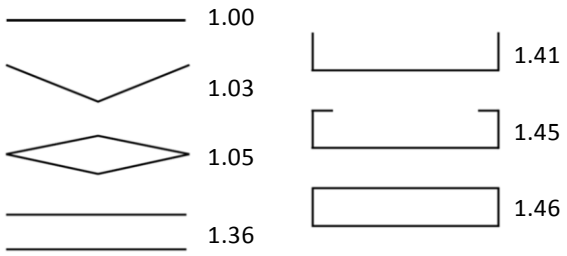

Figure 3. Ideal span efficiency (induced drag of the planar wing/induced efficiency of the non-planar wing) of various non-planar wing systems with 20% height/span. All wing systems have equal span and total lift. Adapted from Kroo[2].

Small scale propeller testing

An important purpose of the present study was to decide whether rapid prototyping and testing of small scale model propellers is of relevance to high-speed applications. The diameter of all propellers manufactured and tested was 150 mm.

The availability of empirical data from small scale high-speed propeller tests is limited. Most of the research carried out in the 1980s involved propeller model diameters greater than 600 mm. However, in a recent study from University of Wisconsin[13] an 80 mm diameter model of GE36 is used for aeroacoustic experiments. For low-speed applications, such as Unmanned Aerial Vehicles and model aircraft, University of Illinois provides a database covering wind tunnel tests of more than 100 propellers[14], which has been used in the present study for initial test rig evaluation.

Design considerations

Following the principles of technology readiness level[15] (TRL) for describing the maturity of a new technology, the joined-blade propeller work started at TRL 1-2 aiming at proofing the concept by experiments and numerical analysis.

The overall objectives for the work described in this article can be summarized as,

1. To demonstrate that forward-swept high-speed joined-blade propellers are mechanically and aerodynamically feasible.
2. To identify any specific issues related to mechanical integrity and deformation as well as performance.
3. Show that small scale manufacturing and testing provide relevant data for the development process and in general constitutes a poss-ible way forward at low TRL.

Propeller geometry and layout

The first step in the geometry layout of the joined-blade pro-peller was to parameterize the stacking line by introducing a new parameter *s* varying from -1 at the first blade root, 0 at the blade tip and 1 at the other blade root thus allowing a continuous parameterization of the complete blade pair, see example layouts in figure 4 and 5.

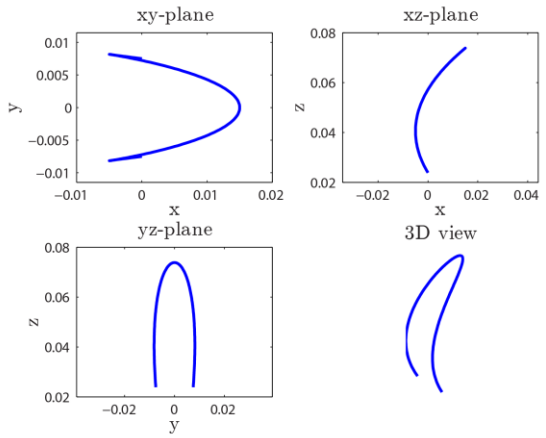

Figure 4. Stacking line example [m].

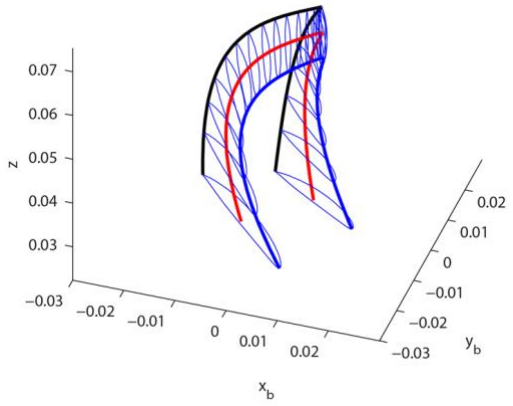

Figure 5. Example of propeller blade geometry generation in Matlab [m].

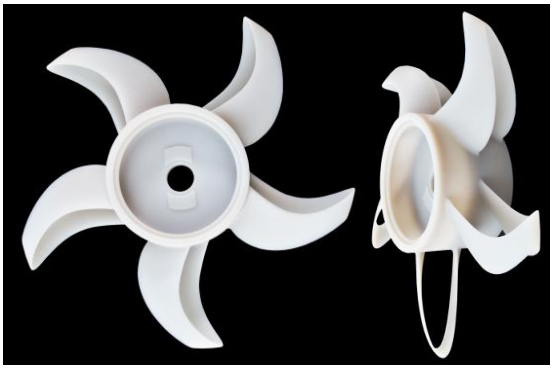

Figure 6. GPX313 front and side view.

Prototype manufacturing

The propellers used for the initial experiments were manufactured by a rapid prototype supplier in Sweden. One of the early questions that were raised was whether 3D printing could be a suitable process for functional prototypes of propellers at low TRLs in early product development. Initially, two diff- erent processes were evaluated and compared, fused deposition modeling (FDM) and the PolyJet process. The FDM process works by heating a thermoplastic material to a semi-liquid state and extruding it layer by layer onto a support material. In the PolyJet process a liquid photopolymer is sprayed onto a support material, layer by layer and cured by UV light. Some important material characteristics are provided in table 1.

Material	Ultem 9085	VeroGray RGD850	80%Carb./ 20%S-Glass (GE36)
Method	FDM	PolyJet	N/A
Spec. Strength [MPa*cm^3/g]	54-63	43-55	390
Spec. stiffness [MPa*cm^3/g]	1700-2600	1700-2500	38000
Min. layer thickness [mm]	0.25	0.016	N/A
Min. airfoil thickness [mm]	~1	~1	N/A

Table 1. Strength and stiffness for the FDM and PolyJet materials available for this study[16,17]. The GE36 fan blade material strength properties are given along the blade[6].

Based on the smoother surface of the VeroGray propeller, the decision was to continue with the PolyJet process for the remainder of the prototype manufacturing.

Joined-blade propeller prototypes

The three tested prototypes have a diameter of 150 mm and main design parameters as given in table 2. The propeller blade airfoils are based on the NACA 16 series. The design objective was to use the sweep angle and total activity factor representative of the state-of-the-art high-speed propellers of the 1980s[6]. However, the thickness to chord ratio could not be reduced below 7% due to the rapid prototyping process constraints. This can be compared to the 2% thickness at the fan blade tips of GE36[6].

Prop.	blades	AF [-]	Pitch [deg]	Sweep [deg]
GPX100	5	1800	26	~50
GPX313	5	1800	26	~50
GPX404	5	1800	20	~40

Table 2. Joined-blade propeller prototypes tested. Sweep refers to the maximum sweep angle near the tip.

At this early stage in the development it is important to realize that the propellers do not represent any efficiency maximum or the best final mechanical design. Instead, these joined-blade propellers should be looked at as first prototypes giving the basics of how they behave mechanically and performance wise. For instance, known 3D aerodynamic effects are not considered in the design, neither is the interaction with an aft rotor. This work was solely focused on the single propeller properties but preparing for the next step which is the counter-rotating joined-blade propeller design.

Experimental set-up

The propellers were tested in a static test rig at Chalmers University of Technology that was designed and built, mainly from COTS components, for the purpose of this work. The overall rig design is shown in figure 7 and 8. The rig is designed for continuous operation at maximum rated power at 32000 RPM for 120 seconds. The propeller drive consists of a brushless DC engine rated at 10 kW shaft power supplied by up to four 12V batteries with a capacity of 100 Ah each. The maximum propeller diameter for this rig is approximately 0.5 m. Measured quantities are thrust, rotational speed, current, voltage and ambient conditions in terms of pressure and temperature. The load cells for thrust measurement are calibrated with a static load.

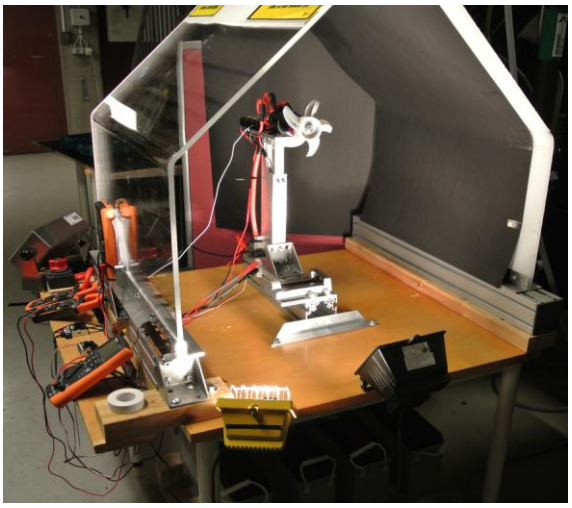

Figure 7. Static propeller rig at Chalmers University of Technology.

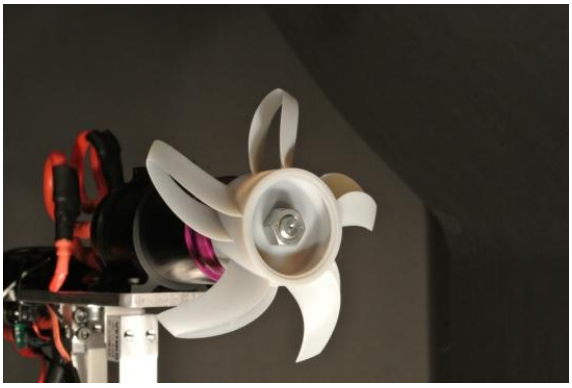

Figure 8. The GPX313 propeller mounted in the static test rig (aft view).

Analysis

Mechanical Strength

The linear FE stress analysis of the initial GPX100 propeller showed relatively high stress concentrations on the inner surface of the joined-blade tips, see figure 9. The results showed von Mises stress levels exceeding 200% of the UTS for the VeroGray material.

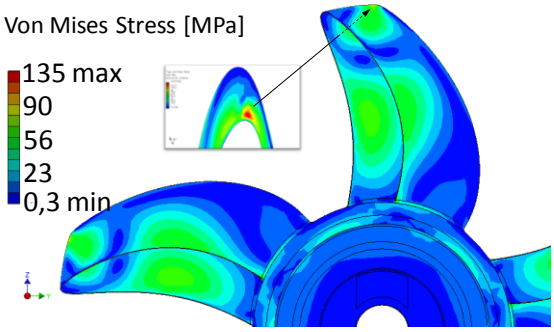

Figure 9. Von Mises Stress levels due to centrifugal loads of the GPX100 propeller at the design point.

After some modifications of the blade geometry to better approximate the blade catenary line, the max von Mises stress of the GPX313 propeller was reduced to approximately 80% of the UTS, giving a safety factor of 1.2, see figure 10.

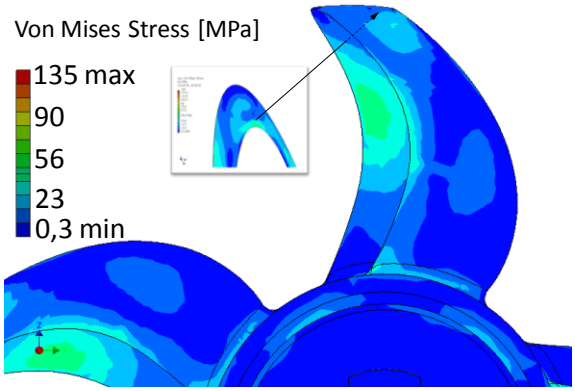

Figure 10. Von Mises Stress levels due to centrifugal loads of the GPX313 propeller at the design point.

Aerodynamic performance

The flow around one box blade of the GPX313 was simulated to achieve an improved understanding of the flow physics and provide input for geometrical improvements. The flow 1.3 blade heights upstream and 1.7 heights downstream of the blade was calculated in 3-D and the far-field in 2-D. Calculations used ANSYS CFX with a k-ω based shear stress transport turbulence model and unstructured grids with 2 to 38 million elements. Calculations were done at two inflow velocities cor-

responding to J=0.15 and 0.77. The thrust results varied less than 2% for grids with at least 9 million elements and for a range of domain sizes. Accurate simulation of static performance may require a larger domain due to recirculation, and has not been performed yet.

Figure 11 illustrates the flow on cylindrical surfaces. At the 75% radius used to define the nominal pitch, the airfoils act fairly independently. At 95% radius the interference causes an increase of the Mach number and an associated low pressure between the blades. The Mach number is limited below 0.82 around the entire blade, a result which is favorable when increasing the flight speed, and is likely due to the blade sweep. The thrust distribution between the upstream and downstream blade half was checked and found to be almost equal at J=0.77. At J=0.15, for this fixed pitch propeller, about 60% of the thrust comes from the downstream blade.

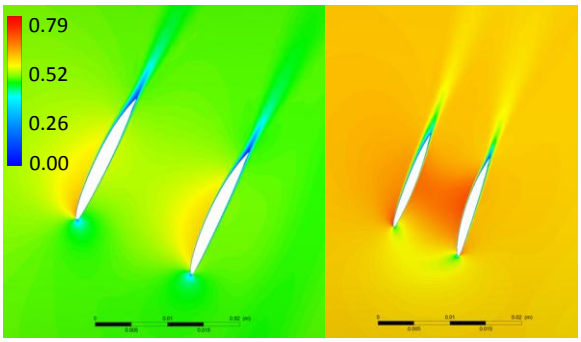

Figure 11. GPX313, blade relative Mach number at 75% radius (left) and 95% radius (right). J=0.77, the rotational axis is horizontal.

Experimental results

The test results indicated thrust coefficients falling with increased speed for the GPX100, see figure 12. In terms of static propeller performance this is fairly atypical, especially for low Reynolds number tests, where increasing speeds is expected to give thinner boundary layers and increased thrust. In contrast, the mechanically improved GPX313 and 404 yielded rising C_T curves. It is possible that mechanical deformation caused the falling values for GPX100.

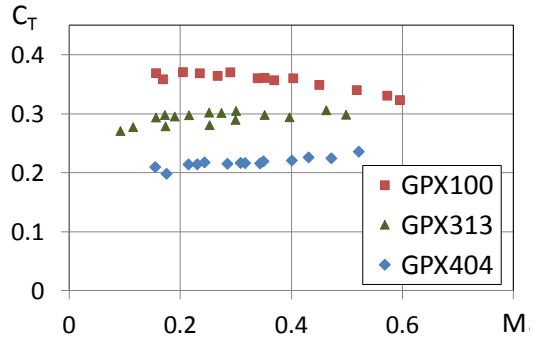

Figure 12 Experimental static thrust coefficient vs. tangential tip Mach number.

The GPX313 thrust coefficient increased 77% when reducing the advance ratio from 0.77 to 0.15, see figure 13. It is likely that static simulations would yield somewhat higher thrust than at J=0.15, and thus higher than seen in experiments. This may be due to simulating smooth surfaces, whereas the experiments are done with unimproved surfaces from the PolyJet process, which has steps, just visible to the eye, stemming from the 0.02 mm layer thickness. Deformation during rotation may also reduce thrust. Further, it is possible that the turbulence model used in the simulation under predicts flow separation, which affects thrust at low advance ratios.

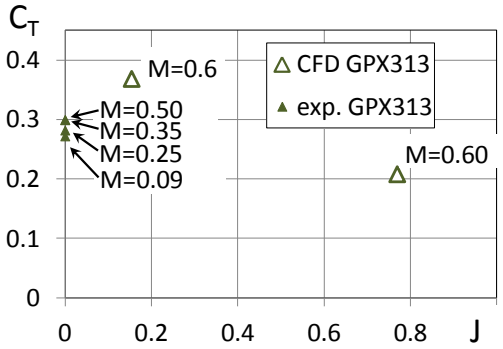

Figure 13. Thrust coefficient vs. advance ratio for tests and flow simulations.

Conclusions

Although still very early in the research and development process of the first joined-blade propeller it is possible to make some interesting conclusions. Through careful mechanical design of the joined-blades, and via the high-speed propeller tests at Chalmers University, it is concluded that rapid prototyping manufacturing methods using moderate strength polymeric materials is an interesting alternative for functional high-speed propeller testing at low technology readiness levels.

Furthermore, based on the positive outcome of the experimental work described in this article, the next development step can be started by initiating the design of the counter-rotating Boxprop and wind tunnel test stand to proof the concept at TRL 3.

Acknowledgements

This work was partially funded by Chalmers University of Technology in Gothenburg, Sweden. The experimental work was carried out at the Division of Fluid Dynamics, Department of Applied Mechanics at Chalmers University under the auspices of Dr Valery Chernoray and Professor Tomas Grönstedt.

The authors would also like to thank the ambitious thesis workers Anna Lind, Fredric Carlsvärd, Johan Olofsson, Samuel Adriansson and Viktor Pettersson that have performed the analysis and testing described in this article.

References

[1] Prandtl, L., 1924, *Induced drag of multiplanes*, NACA TN-182.

[2] Kroo, I., 2005, *Nonplanar wing concepts for increased aircraft efficiency*, VKI Lecture Series on Innovative Configurations and Advanced Concepts for Future Civil Aircraft, June 6-10, 2005.

[3] Boeing, 2009, *Sweeping Changes*, Boeing Frontiers, Vol. VII, Iss. X, March 2009.

[4] Hepperle, M., 2008, *MDO of Forward Swept Wings*, Presentation for the KATnet II Workshop, Braunschweig, Germany, 28-29 Jan, 2008.

[5] Seitz, A. et. al., 2011, *The DLR Project LamAiR: Design of a NLF Forward Swept Wing for Short and Medium Range Transport Application*, AIAA 2011-3526.

[6] GE36 Systems Engineering and Design, 1987, *Full scale Technology Demonstration of a modern counterrotating unducted fan engine concept*, NASA CR-180867, NASA Lewis Research Center, Dec 1987.

[7] Woodward, R. et. al., 1991, *Take-off/Approach Noise for a Model Counter-rotation Propeller with a Forward Swept Upstream Rotor*, NASA TM-105979, AIAA-930596.

[8] Avellán, R. & Lundbladh, A., 2011, *Air Propeller Arrangement and Aircraft*, International Patent Application WO2011/081577A1, filed on Dec 28, 2009.

[9] Avellán, R. & Lundbladh, A., 2012, *Air Propeller Arrangement and Aircraft*, US Patent Application US2012/0288474A1, filed on Dec 28, 2009.

[10] Korkan K. D. & Gregorek, G. M., 1980, *An Acoustic Sensitivity Study of General Aviation Propellers*", AIAA-80-1871.

[11] Jeracki, R.J., & Mitchell G.A., 1981, *Low and High Speed Propellers for General Aviation – Performance Potential and Recent Wind Tunnel Test Results*, NASA TM-81745.

[12] Hartzell Propellers Inc., URL: http://www.hartzellprop.com, cited on 25 April, 2013.

[13] Truong, A. & Papamoschou, D., 2013, *Aeroacoustic Testing of Open Rotors at Very Small Scale*, AIAA-2013-0217.

[14] Brandt, J.B. & Selig, M.S., 2011, *Propeller Performance Data at Low Reynolds numbers*, AIAA-2011-1255.

[15] Mankins, J. C., 1995, *Technology Readiness Levels – a white paper*, NASA, 6 Apr 1995.

[16] SABIC, 2013, *Innovative Plastics LITHWEIGHT+ COMPLIANT Next Generation Solutions for Aircraft Designers*, SABIC-PLA-4036-EN.

[17] STRATASYS Ltd., 2012, *Objet Materials Data Sheets - VeroGray RGD850*.